Review of Scientific Instruments

Improvement of the performances of a commercial hand-held laser-induced breakdown spectroscopy instrument for steel analysis using multiple artificial neural networks

Cite as: Rev. Sci. Instrum. **91**, 073111 (2020); https://doi.org/10.1063/5.0012669
Submitted: 03 May 2020 . Accepted: 06 July 2020 . Published Online: 24 July 2020

F. Poggialini, B. Campanella, S. Legnaioli, S. Pagnotta, S. Raneri, and V. Palleschi

View Online Export Citation CrossMark

ARTICLES YOU MAY BE INTERESTED IN

New algorithm using L1 regularization for measuring electron energy spectra
Review of Scientific Instruments **91**, 075116 (2020); https://doi.org/10.1063/1.5144897

Measurement of the heat flux normalized spin Seebeck coefficient of thin films as a function of temperature
Review of Scientific Instruments **91**, 073910 (2020); https://doi.org/10.1063/5.0007989

Hall effect instruments, evolution, implications, and future prospects
Review of Scientific Instruments **91**, 071502 (2020); https://doi.org/10.1063/5.0009647

MCL MAD CITY LABS INC. www.madcitylabs.com
Nanopositioning Systems
Modular Motion Control
AFM and NSOM Instruments
Single Molecule Microscopes

© 2020 Author(s).

AIP Publishing

Review of Scientific Instruments ARTICLE scitation.org/journal/rsi

Improvement of the performances of a commercial hand-held laser-induced breakdown spectroscopy instrument for steel analysis using multiple artificial neural networks

Cite as: Rev. Sci. Instrum. 91, 073111 (2020); doi: 10.1063/5.0012669
Submitted: 3 May 2020 • Accepted: 6 July 2020 •
Published Online: 24 July 2020

View Online Export Citation CrossMark

F. Poggialini,[1,2] B. Campanella,[1] S. Legnaioli,[1] S. Pagnotta,[3] S. Raneri,[1] and V. Palleschi[1,a)]

AFFILIATIONS

[1]Applied and Laser Spectroscopy Laboratory, Institute of Chemistry of Organometallic Compounds, Area della Ricerca del CNR, Via G. Moruzzi, 1, 56124 Pisa, Italy
[2]Scuola Normale Superiore, Piazza dei Cavalieri, 7-56126 Pisa, Italy
[3]Earth Science Department, University of Pisa, Via S. Maria, 53, 56126 Pisa, Italy

[a)]**Author to whom correspondence should be addressed:** vincenzo.palleschi@cnr.it

ABSTRACT

In this article, we present a study on the optimization of the analytical performance of a commercial hand-held laser-induced breakdown spectroscopy instrument for steel analysis. We show how the performances of the instrument can be substantially improved using a non-linear calibration approach based on a set of Artificial Neural Networks (ANNs), one optimized for the determination of the major elements of the alloy, and the others specialized for the analysis of minor components. Tests of the instrument on steel samples used for instrument internal calibration demonstrate a comparable accuracy with the results of the ANNs, while the latter are considerably more accurate when unknown samples, not used for calibration/training, are tested.

Published under license by AIP Publishing. https://doi.org/10.1063/5.0012669

I. INTRODUCTION

The recent introduction of the hand-held laser-induced breakdown spectroscopy (HH-LIBS) instruments has been unanimously seen by the community working in LIBS as a breakthrough toward a larger diffusion of the technique in the fields where it works better, i.e., industrial or, in general, out-of-the-lab applications.[1] In fact, the need for compacting in a hand-held instrument a power laser, a wide-band spectrometer, a computer for the elaboration of the data, and all the optics and electronics has forced the major producers of these instruments to compromise on some things, which unavoidably degrade the performance of these systems. Despite that, several interesting results have been obtained in recent years on applications of hand-held LIBS instruments to geological materials,[2–6] precise agriculture,[7] metallurgy,[8–11] industrial processes,[12] nuclear industry,[13] and cultural heritage.[2,14]

It is commonly accepted that the intrinsic limitations of hand-held LIBS instruments may be partially overcome using advanced chemometric tools for the quantitative analysis of the spectra.[5–7,15] On the other hand, the complexity of the analysis should be reasonable for the LIBS data to be processed by the low computational power computers controlling these instruments. In this paper, we will show how the optimization of the analytical procedure may improve considerably the performances of a hand-held LIBS instrument without introducing unreasonable loads on the internal computer.

II. MATERIALS AND METHODS

The LIBS hand-held instrument used in this work is the EOS 500 HH-LIBS instruments by Bruker, Nano Inc., USA. The EOS 500

Published under license by AIP Publishing

is a lightweight instrument (2.4 kg including battery); it uses a proprietary Nd:YAG laser at 1064 nm with a repetition rate of 5 kHz, an average power of around 100 mW, and a power density on the sample >1 GW/cm^2. The multi-detector design covers the wavelength range from 170 nm to 720 nm with a resolution of about 0.15 nm. The spot of analysis (about 100 μm in diameter) is rastered across the surface to avoid the formation of deep craters and increase the representativity of the analysis. The sampled area in a measure is about 1 mm^2.

The instrument tested was specifically calibrated at the factory for the analysis of steel. A set of samples used for the instrument calibration (32 certified steel samples) were made available to us by Bruker (see Table I) so that the performances of the internal software of the instrument could be easily compared with the ones based on a different multivariate approach.

To study the possible improvement in the analytical performances of the EOS 500 instrument (without intervening on the hardware), we tested a solution based on the application of simple Artificial Neural Networks (ANNs).[16] The use of artificial neural networks in LIBS analysis is now largely consolidated; after the early works of Motto-Ros *et al.*,[17–19] many papers using ANNs for classification[20–23] and quantification[24,25] of LIBS spectra have been published. Hybrid quantification methods have been also proposed.[26,27] The main advantage of the ANN approach with respect to other uni- and multi-variate approaches is the capability of representing well the complex non-linear dependence between the signal and sample composition, which is typical of LIBS analysis.

The ANN algorithm links a set of inputs (in our case, the spectral intensities of some lines in the LIBS spectrum) to a set of outputs (in our case, the concentration of the elements of interest) through a non-linear relation that can be determined by minimizing the deviation between the predicted and nominal outputs on a set of known samples. The relation obtained between inputs and outputs is then used for obtaining the outputs associated with unknown samples from the measured inputs.

The algorithms for building an ANN are powerful and robust, and software packages are available, which make their application

TABLE I. Composition of the certified steel samples used for training the ANNs (all the concentrations are in wt. %).

	Fe	C	Si	Al	V	Mn	Cu	Ni	Cr	Mo
Iron	99.92	0.002	<0.1	0.002	1×10^{-3}	1×10^{-3}	0.004	0.004	0.001	0.002
c1018	98.24	0.2	0.21	0.003	0.006	0.69	0.25	0.1	0.15	0.03
c1117	97.87	0.2	0.15	0.002	0.003	1.13	0.17	0.08	0.17	0.01
c4140	96.6	0.43	0.27	0.0219	0.004	0.9	0.22	0.19	1.05	0.18
c4340	95.54	0.41	0.22	0.036	0.004	0.75	0.19	1.66	0.85	0.22
c4620	96.57	0.21	0.26	0.026	0.003	0.58	0.1	1.77	0.15	0.24
c6150	96.88	0.51	0.22	0.014	0.17	0.78	0.18	0.14	0.99	0.04
c8620	97.34	0.2	0.23	0.003	0.068	0.8	0.12	0.49	0.45	0.18
e52100	96.56	1.04	0.26	0.003	0.004	0.33	0.13	0.1	1.47	0.02
Cr1.25	96.77	0.12	0.61	0.001	0.02	0.52	0.08	0.09	1.23	0.49
Cr2.25	95.7	0.1	0.22	0.003	0.008	0.55	0.17	0.16	2.07	0.93
P5	94.04	0.133	0.25	0.004	0.012	0.46	0.13	0.1	4.27	0.46
P9	88.89	0.13	0.38	0.004	0.02	0.41	0.15	0.24	8.66	0.96
303	71.22	0.061	0.37	<0.001	0.048	1.6	0.4	8.11	17.18	0.36
304	71.28	0.057	0.56	<0.001	0.092	0.66	0.33	8.21	18.41	0.19
309	61.92	0.076	0.43	0.012	0.06	1.58	0.31	12.48	22.54	0.36
310	51.31	0.068	0.53	0.01	0.1	1.69	0.3	20.05	25.48	0.15
321	68.51	0.046	0.57	0.023	0.14	1.95	0.18	10.16	17.41	0.37
330	41.75	0.063	1.24	0.022	0.05	1.51	0.19	35.53	19	0.31
316	67.82	0.053	0.59	<0.001	0.09	1.61	0.4	10.29	16.75	2.1
347	69.16	0.057	0.77	0.017	0.06	1.48	0.1	9.93	17.41	0.17
410	86.5	0.14	0.29	0.002	0.05	0.54	0.07	0.39	11.84	0.07
416	85.29	0.12	0.53	0.002	0.04	0.8	0.13	0.4	12.18	0.12
430	81.74	0.042	0.51	<0.001	0.04	0.4	0.13	0.22	16.8	0.02
431	80.18	0.14	0.37	0.076	0.07	0.61	0.1	2.27	16.03	0.07
440C	80	1.09	0.41	<0.001	0.04	0.39	0.09	0.22	17.07	0.52
446	74.59	0.089	0.37	<0.001	0.045	0.46	0.06	0.31	23.84	0.05
TS O-6	96.09	1.39	1.02	0.011	0.005	0.89	0.05	0.11	0.13	0.25
TS A-6	94.47	0.68	0.25	0.009	0.007	2.15	0.09	0.14	1.04	1.05
TS S-5	95.15	0.58	1.92	0.017	0.22	0.8	0.25	0.23	0.29	0.41
TS S-1	94.12	0.49	0.94	0.011	0.16	0.48	0.08	0.3	1.31	0.16
TS M-2	80.38	0.86	0.39	0.027	1.86	0.31	0.14	0.2	4.25	5.08

Published under license by AIP Publishing

easy. The obvious disadvantage of the ANN approach is the need for many representative samples to be used for the calibration and the length of the training procedures. It should be stressed, however, that the training of the ANN can be performed in the laboratory with the help of fast computers, while the quantitative analysis of the acquired spectra could be easily managed by the low computational power computer of the hand-held instrument, using the parameters of the ANN previously determined.

The 32 certified steel samples used for building the ANNs used in this work were provided from ARMI MBH/LGC Standards, Manchester, NH, USA, and were kindly given to us by Bruker (see Table I).

We acquired 15 spectra per sample (480 spectra in total) for training the neural network. A typical LIBS spectrum, acquired by the EOS 500 HH-LIBS instrument, is shown in Fig. 1.

One of the most important strategies in multivariate analysis is the reduction of the number of inputs (or predictors) for the analysis. In the case of LIBS, one must often deal with thousands of spectral data; this number must be reduced to avoid the problem of overfitting, i.e., the use of more variables than the degrees of freedom of the multivariate model. The feature selection can be obtained using several simplification techniques. The most obvious is the manual selection of the spectral points corresponding to the main emission lines of the elements to be determined[24,28] or the use of their integral or peak intensities,[29] but it can be unpractical in the presence of elements, as Fe in the steel, which emit hundreds of lines in the spectral range considered. Alternatively, automated methods such as Principal Component Analysis (PCA),[30] Genetic Algorithms (GAs),[31] Forward Feature Selection (FFS),[16] and other similar techniques[32,33] can be applied. In our case, the feature selection was done based on the ratio between the standard deviation and the average of the spectra acquired on all the calibration standards. We selected as inputs of the ANN, among the 3681 points of the LIBS spectrum, only the spectral points whose relative standard deviation with respect to the average of all the spectra acquired on the calibration samples was higher than a given fraction T of the maximum (T < 1), as described in the following equation:

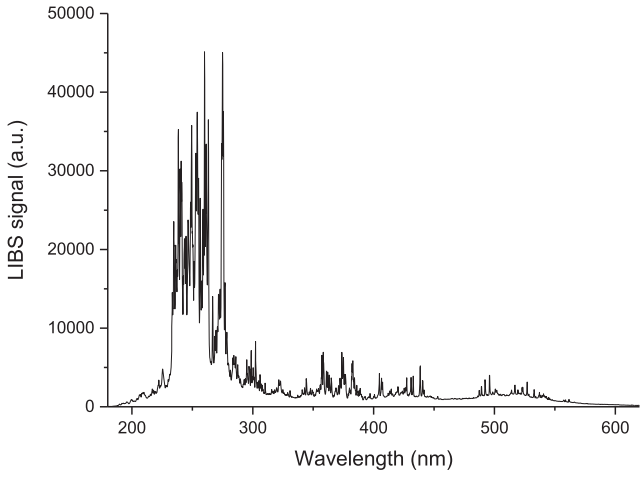

FIG. 1. LIBS spectrum acquired with the EOS 500 (sample c1018).

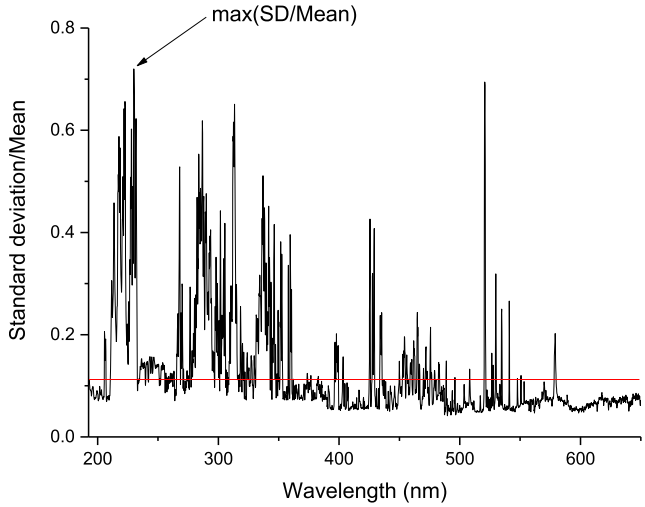

FIG. 2. Feature selection for the ANN. The spectral inputs are chosen in correspondence to the wavelengths for which the relative standard deviation with respect to the average is larger than 15% (red line in the graph) of the maximum.

$$\frac{SD(I)}{Mean(I)} \geq T * \max\left(\frac{SD(I)}{Mean(I)}\right). \quad (1)$$

In other words, we chose the spectral point that showed the largest variability among the different samples, i.e., the most significant for quantitative analysis and, eventually, classification of the samples. The method is very quick, conceptually equivalent to PCA (the variables that explain the largest variance of the data are retained) and has the further advantage to allow a quick "visual" check on the lines that are included in the analysis as a function of the chosen tbhreshold.

Setting empirically a threshold T = 0.15, we obtain a reduction of about 90% of the spectral inputs (451) with respect to the total number of points of the LIBS spectrum (3681) (see Fig. 2). A quick *a posteriori* check confirmed that all the main emission lines of the elements of interest were included among the inputs.

TABLE II. Composition of the certified steel samples used for testing the ANNs (all the concentrations are in wt. %). We acquired three spectra per test sample (30 spectra in total).

	C	Si	Mn	Cr	Ni	Mo	Co
S1	0.092	0.46	0.74	12.35	12.55	<0.01	<0.01
S2	0.0103	0.374	0.686	14.727	6.124	0.0138	<0.01
S3	0.0345	0.463	0.722	11.888	12.85	0.0304	<0.01
S4	0.019	0.27	1.4	18.46	10.2	0.265	0.116
S5	0.086	0.57	0.791	25.39	20.05	<0.01	0.054
S6	0.066	0.405	1.38	17.31	9.24	0.092	0.053
S7	0.0141	0.48	1.311	17.84	10.2	2.776	0.0184
S8	0.143	1.41	1.7	17.96	8.9	<0.01	0.018
S9	0.05	0.21	0.89	14.14	5.66	1.59	0.22
S10	0.0201	0.537	1.745	16.811	10.72	2.111	0.0525

Published under license by AIP Publishing

The same spectral regions were selected for the analysis of the test samples.

As discussed in Ref. 34, for the analysis of the major components in the alloy (Cr and Ni, besides Fe) and an estimate of the concentration of the minor elements, a ANN was built using ten hidden neurons (corresponding to the number of the elements considered), with a sigmoid activation function. The ANN was built and trained using the package included in Matlab® (ver. 2020a). This ANN was not expected to perform well for the minor elements (Mo, Mn, Si and C, in our case) because it was not specifically optimized for the analysis of the low-concentration elements. In fact, the ANN training algorithm tries to minimize the sum of the absolute deviations with respect to the predicted values for all the elements at the same time. Therefore, the relative errors are higher for the elements at lower concentration. We then analyzed the minor components in the alloy using separate ANNs, each one optimized for refining the analysis of the corresponding element. These networks had the same inputs as the first one, but only one output (in our case, the concentration of the minor element) and only one neuron in the hidden layer.

The results obtained by the ANN on the steel samples used for instrument internal calibration (not shown here for brevity) for the main elements showed a good agreement with the nominal results and the results obtained using the EOS 500 HH-LIBS instrument, which is not surprising since those samples were used both for the internal calibration of the instrument and for the training of the ANN.

For testing and comparing the performances of the ANN with the built-in calibration of the Bruker instrument, as well as excluding the possible occurrence of overfitting, we used ten certified steel samples, specially provided by BAM, Berlin for the proficiency test organized in the occasion of the fifth International LIBS Conference in Berlin, Germany (2008).[35] The composition of the standards is reported in Table II. The BAM standards were not used for training

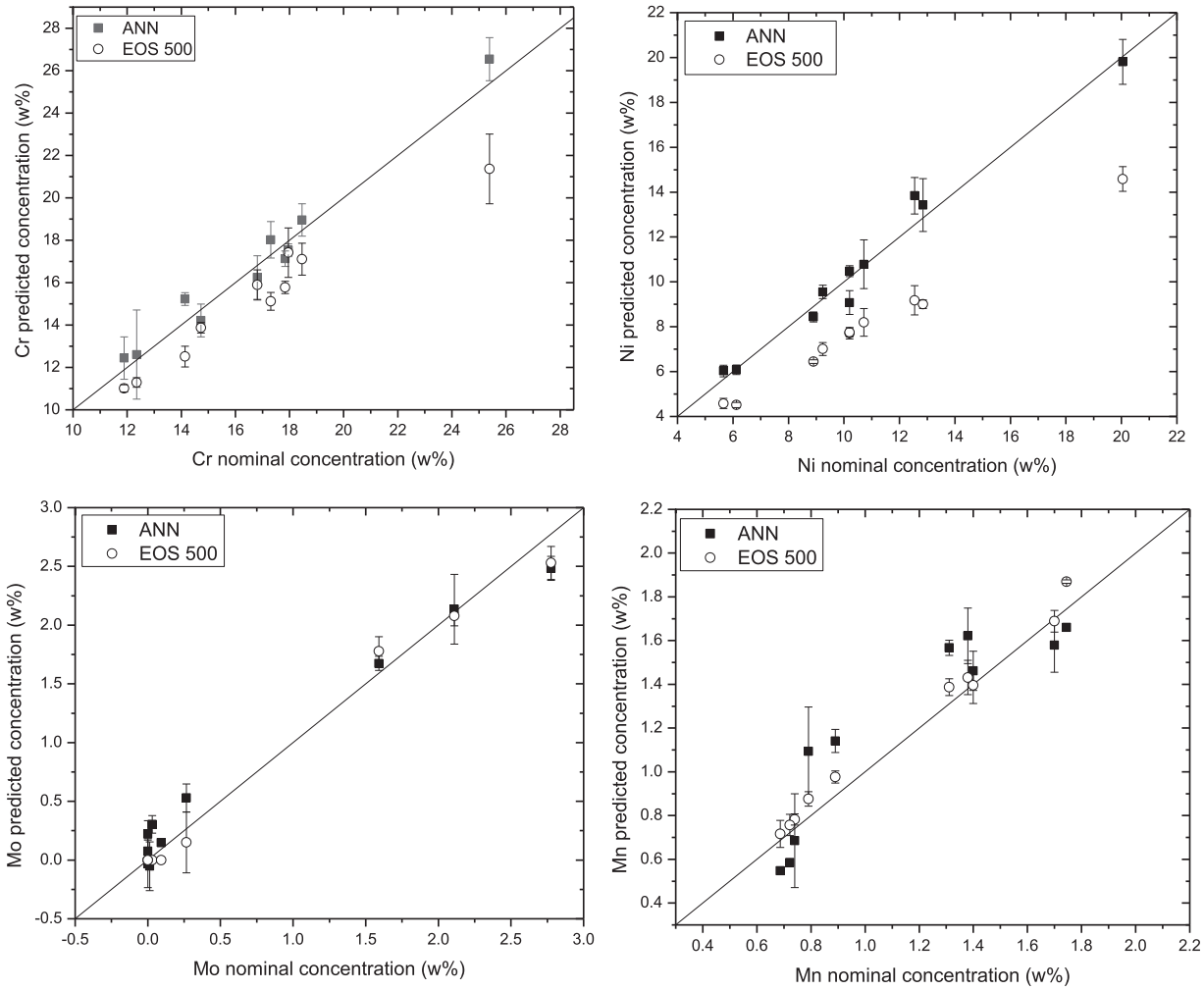

FIG. 3. Comparison between the predicted concentration and nominal ones, for ANN (black squares) and EOS 500 internal calibration (open dots).

Published under license by AIP Publishing

the ANNs or for the internal calibration of the instrument; therefore, the conditions were ideal for comparing our simple model with the EOS 500 internal calibration algorithm.

The elements considered for the analysis were Cr, Ni, Mo, Mn, Si, and C. The Co concentration was not determined because this element was not present in the standards we used for training the ANNs.

III. EXPERIMENTAL RESULTS

The comparison of the results obtained from the ten test samples with the ANN designed for the analysis of the major elements is shown in Fig. (3). The points correspond to the average of the three independent acquisitions, and the error bars represent the corresponding standard deviations. In Fig. 3, the continuous line represents the 1:1 correspondence between nominal and measured concentrations for the given element.

In Table III, we report the slope of the best linear fit curves of the experimental data for the elements in Fig. 3, the coefficient of determination R^2 of the fit, the Root Mean Standard Error (RMSE), and the average bias b of the data, defined as

$$R^2 = \frac{(\sum_i (y_i - \bar{y})(x_i - \bar{x}))^2}{\sum_i (y_i - \bar{y})^2 \sum_i (x_i - \bar{x})^2},$$
$$\text{RMSE} = \sqrt{\frac{\sum_i (y_i - Y_i)^2}{N}}, \quad (2)$$
$$b = \frac{\sum_i (y_i - Y_i)}{N},$$

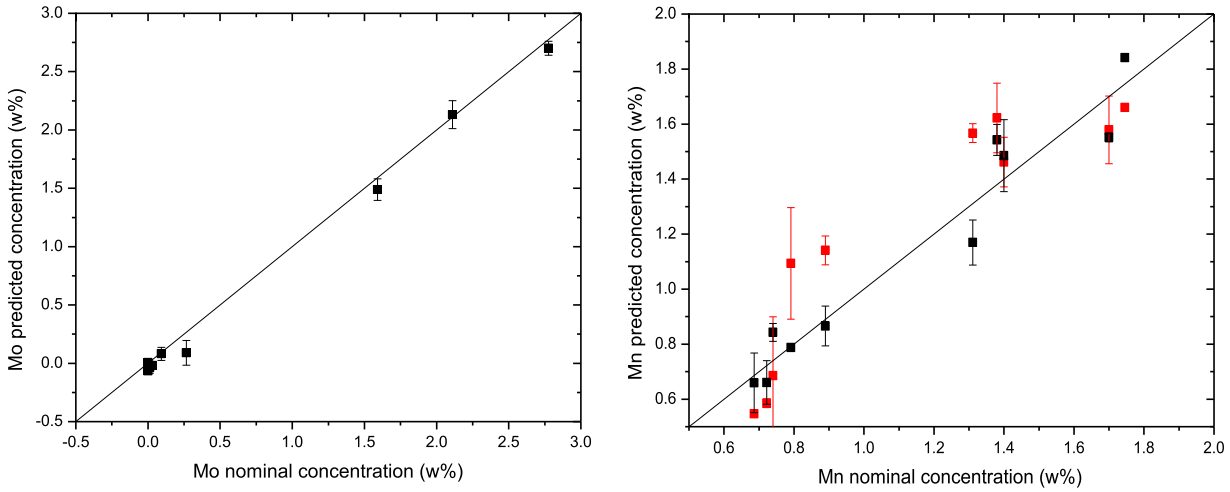

FIG. 4. Comparison between the predicted concentration and nominal ones, for the two specialized ANNs (Mo at the left and Mn at the right). The black line corresponds to the 1:1 coincidence of the predicted and nominal concentrations. The red points in the Mn graph correspond to the prediction of the ANN for the main elements.

TABLE III. Comparison of the performances of ANN and internal EOS 500 calibration for the four elements considered.

	ANN				EOS 500			
	Slope	R^2	RMSE (wt. %)	b (wt. %)	Slope	R^2	RMSE (wt. %)	b (wt. %)
Cr	1.00	0.999	0.70	0.2	0.913	0.999	1.83	−1.55
Ni	1.00	0.997	0.62	0.10	0.73	0.999	2.98	−2.75
Mo	0.984	0.973	0.19	0.06	0.967	0.992	0.11	−0.03
Mn	0.901	0.773	0.05	0.08	1.06	0.999	0.07	0.05

	ANN 2			
	Slope	R^2	RMSE (wt. %)	b (wt. %)
Mo	0.997	0.997	0.05	−0.11

	ANN 3			
	Slope	R^2	RMSE (wt. %)	b (wt. %)
Mn	1.01	0.933	0.1	−0.03

Published under license by AIP Publishing

where x_i are the nominal concentration, y_i are the estimated concentration, $\bar{x}$ and $\bar{y}$ are their averages, and N is the number of test samples analyzed (N = 10 in our case).

From the analysis of the figures of merit reported in Table III, it appears clearly that the ANN gives much better results (slope and R^2 close to 1, lower RMSE and average bias) than the EOS 500 internal calibration for Cr and Ni. As anticipated, the results for the minor elements are comparable (Mo) or worse than the EOS 500 internal calibration (Mn). The results for C and Si were comparably poor/absent for both the main ANN and the EOS internal calibration.

The results of the specialized ANNs for Mo and Mn are shown in Table III and Fig. 4.

The predictions of the specialized ANNs are more precise than the ones of the main ANN. This is clear but marginal for Mo, which was already managed by the main ANN with a precision comparable with the internal calibration of the EOS 500 instrument. The improvement is more marked for manganese, although the scatter of the data is still important. However, the analytical factors of merit of the calibration are now comparable with that of the internal calibration of the instrument.

Specialized ANNs were also built for Si and C. The quantification of Si in steel is more problematic with respect to Mo and Mn because in the LIBS spectrum only a few intense Si emission lines can be observed, which are interfered by the emission lines of the major elements Ni and Cr.[36] Nevertheless, using the specialized ANN, a quantitative determination of Si in the test samples can still be obtained, as shown in Fig. 5.

The internal calibration of EOS 500 had a Limit of Detection (LOD) for Si of 0.5 wt. %. The ANN predictions are slightly better, but the indetermination on the results is quite large at those concentrations.

The quantification of carbon in steel is even more complex: the C I line at 247.86 nm, which is typically used for carbon quantification, is covered by the neighboring Fe I and Fe II lines; however, the carbon information is still carried by the line at 193.09 nm, which is free from interferences but lies in a spectral region, where the sensitivity of the EOS 500 detector is very low.

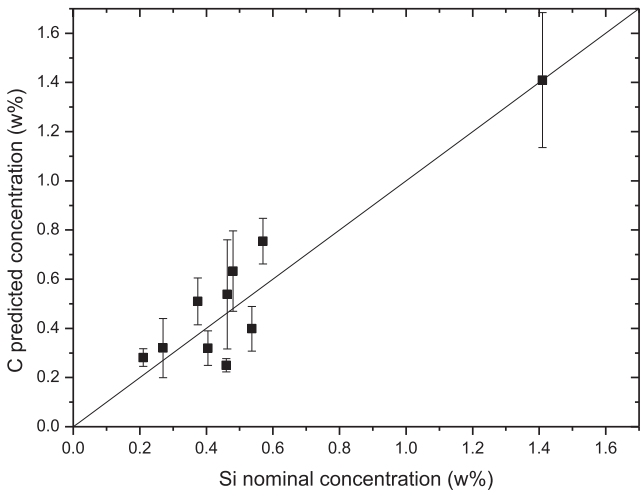

FIG. 5. Comparison between the predicted concentration and nominal ones for the Si specialized ANN. The black line corresponds to the 1:1 coincidence of predicted and nominal concentrations.

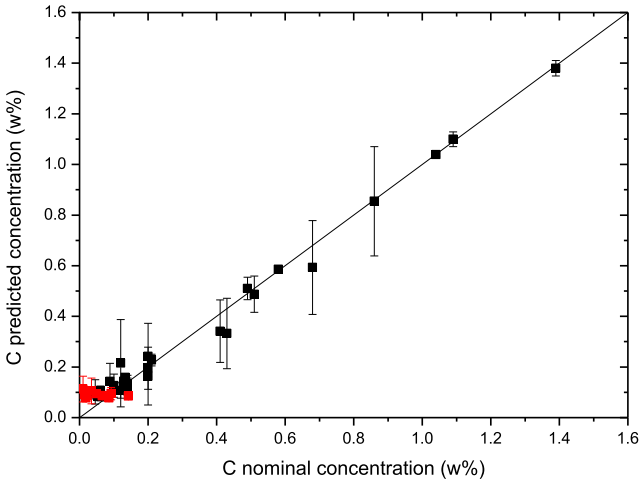

FIG. 6. Comparison between the predicted concentration and nominal ones for the C specialized ANN. The black line corresponds to the 1:1 coincidence of predicted and nominal concentrations. The points in red correspond to the results obtained on the test samples.

In Fig. 6, the comparison is shown between the carbon concentration predicted by the corresponding specialized ANN and the nominal concentration in the standards.

The specialized ANN provides a good quantitative determination of carbon concentration, at least for concentrations above 0.5 wt. %–1 wt. %. This is a good achievement, even compared to benchtop LIBS instrumentation. It should also be considered that the internal calibration of the EOS 500 was not able to give results for carbon, on both the calibration standards and the test samples. In our test steel samples, the nominal concentration of carbon is lower than 0.15 wt. %, well below the limit of quantification of the instrument, and the specialized ANN is just able to confirm that the concentration is below 0.2 wt. % for all the samples.

It is worth to note again that, once properly trained, these specialized neural networks would operate as quickly as the main one, and the whole process of spectral analysis would require a computational power perfectly compatible with a hand-held device.

Given the limited number of standards used for training the ANN (32) and considering that a single ANN was used for the determination of major elements in the samples, the authors feel that the accuracy of the results obtained with the EOS 500 instrument could be substantially improved by simply changing the internal calibration method to an ANN-based algorithm.

IV. CONCLUSION

Hand-held LIBS instrumentation represents the future of LIBS "real world" applications. However, the need for compactness, lightweight, and robustness of HH-LIBS instruments might call for compromises on the analytical performances of the equipment, which should be compensated by a suitable analytical strategy. In

Published under license by AIP Publishing

this communication, we have shown that the choice of a proper calibration algorithm, guided by a sound chemical/physical model of the system, allows us to reach better analytical performances with respect to other more traditional methods; this is even more true, considering that the results obtained were based on a calibration exploiting only 32 certified steel samples.

AUTHORS' CONTRIBUTIONS

All authors contributed equally to this work.

ACKNOWLEDGMENTS

The authors acknowledge Bruker for the use of the EOS 500 instrument and the calibration samples and BAM for providing the steel standards. Part of the activity was funded by a grant from the Italian Ministry of Foreign Affairs and International Cooperation (MACH Project No. RS19GR04).

DATA AVAILABILITY

The data that support the findings of this study are available from the corresponding author upon reasonable request.

REFERENCES

[1] R. Noll, C. Fricke-Begemann, S. Connemann, C. Meinhardt, and V. Sturm, "LIBS analyses for industrial applications—An overview of developments from 2014 to 2018," J. Anal. At. Spectrom. **33**(6), 945–956 (2018).

[2] G. S. Senesi, D. Manzini, and O. De Pascale, "Application of a laser-induced breakdown spectroscopy handheld instrument to the diagnostic analysis of stone monuments," Appl. Geochem. **96**, 87–91 (2018), available from https://linkinghub.elsevier.com/retrieve/pii/S0883292718301641.

[3] G. S. Senesi, P. Manzari, G. Tempesta, G. Agrosì, A. A. Touchnt, A. Ibhi *et al.*, "Handheld laser induced breakdown spectroscopy instrumentation applied to the rapid discrimination between iron meteorites and meteor-wrongs," Geostand. Geoanal. Res. **42**(4), 607–614 (2018).

[4] R. S. Harmon, C. J. M. Lawley, J. Watts, C. L. Harraden, A. M. Somers, and R. R. Hark, "Laser-induced breakdown spectroscopy—An emerging analytical tool for mineral exploration," Minerals **9**(12), 718 (2019).

[5] R. S. Harmon, C. S. Throckmorton, R. R. Hark, J. L. Gottfried, G. Wörner, K. Harpp *et al.*, "Discriminating volcanic centers with handheld laser-induced breakdown spectroscopy (LIBS)," J. Archaeol. Sci. **98**, 112–127 (2018).

[6] Y. Foucaud, C. Fabre, B. Demeusy, I. V. Filippova, and L. O. Filippov, "Optimisation of fast quantification of fluorine content using handheld laser induced breakdown spectroscopy," Spectrochim. Acta, Part B **158**, 105628 (2019).

[7] A. Erler, D. Riebe, T. Beitz, H.-G. Löhmannsröben, and R. Gebbers, "Soil nutrient detection for precision agriculture using handheld laser-induced breakdown spectroscopy (LIBS) and multivariate regression methods (PLSR, Lasso and GPR)," Sensors **20**(2), 418 (2020).

[8] M. S. Afgan, Z. Hou, and Z. Wang, "Quantitative analysis of common elements in steel using a handheld μ-LIBS instrument," J. Anal. At. Spectrom. **32**(10), 1905–1915 (2017), available from http://xlink.rsc.org/?DOI=C7JA00219J.

[9] S. Piorek, "Rapid sorting of aluminum alloys with handheld μLIBS analyzer," Mater. Today: Proc. **10**, 348–354 (2019).

[10] L. Jingyu, C. Kuan, C. Guofei, L. Yangyan, Z. Aijun, and X. Yu, "Quantitative analysis of magnesium and titanium elements in aluminum alloy by handheld laser-induced breakdown spectroscopy," Laser Optoelectron. Prog. **56**(2), 023002 (2019).

[11] L. Brooks and G. Gaustad, "Positive material identification (PMI) capabilities in the metals secondary industry: An analysis of XRF and LIBS handheld analyzers," in *Minerals, Metals and Materials Series* (Springer International Publishing, 2019), pp. 1375–1380.

[12] B. T. Manard, M. F. Schappert, E. M. Wylie, and G. E. McMath, "Investigation of handheld laser induced breakdown spectroscopy (HH LIBS) for the analysis of beryllium on swipe surfaces," Anal. Methods **11**(6), 752–759 (2019).

[13] B. T. Manard, E. M. Wylie, and S. P. Willson, "Analysis of rare earth elements in uranium using handheld laser-induced breakdown spectroscopy (HH LIBS)," Appl. Spectrosc. **72**(11), 1653–1660 (2018).

[14] G. S. Senesi, D. Manzini, and O. De Pascale, "Handheld laser-induced breakdown spectroscopy instrument for the diagnosis of the conservation state of stone monuments," in *IMEKO International Conference on Metrology for Archaeology and Cultural Heritage, MetroArchaeo 2017* (International Measurement Confederation (IMEKO), 2019), pp. 534–536.

[15] D. Syvilay, B. Bousquet, R. Chapoulie, M. Orange, and F.-X. Le Bourdonnec, "Advanced statistical analysis of LIBS spectra for the sourcing of obsidian samples," J. Anal. At. Spectrom. **34**(5), 867–873 (2019).

[16] E. D'Andrea, S. Pagnotta, E. Grifoni, G. Lorenzetti, S. Legnaioli, V. Palleschi *et al.*, "An artificial neural network approach to laser-induced breakdown spectroscopy quantitative analysis," Spectrochim. Acta, Part B **99**, 52 (2014).

[17] V. Motto-Ros, A. S. Koujelev, G. R. Osinski, and A. E. Dudelzak, "Quantitative multi-elemental laser-induced breakdown spectroscopy using artificial neural networks," J. Eur. Opt. Soc.: Rapid Publ. **3**, 08011 (2008).

[18] A. Koujelev, V. Motto-Ros, D. Gratton, and A. Dudelzak, "Laser-induced breakdown spectroscopy as a geological tool for field planetary analogue research," Can. Aeronaut. Space J. **55**, 97–106 (2009).

[19] A. Koujelev, M. Sabsabi, V. Motto-Ros, S. Laville, and S. L. Lui, "Laser-induced breakdown spectroscopy with artificial neural network processing for material identification," Planet. Space Sci. **58**(4), 682–690 (2010).

[20] A. Ramil, A. J. López, M. P. Mateo, and A. Yáñez, "Classification of archaeological ceramics by means of laser induced breakdown spectroscopy (LIBS) and artificial neural networks," in *Lasers in the Conservation of Artworks—Proceedings of the International Conference LACONA 7* (CRC Press, 2008), pp. 121–125.

[21] B. Campanella, E. Grifoni, S. Legnaioli, G. Lorenzetti, S. Pagnotta, F. Sorrentino *et al.*, "Classification of wrought aluminum alloys by ANN evaluation of LIBS spectra from aluminum scrap samples," Spectrochim. Acta, Part B **134**, 52–57 (2017).

[22] A. Ramil, A. J. López, and A. Yáñez, "Application of artificial neural networks for the rapid classification of archaeological ceramics by means of laser induced breakdown spectroscopy (LIBS)," Appl. Phys. A: Mater. Sci. Process. **92**(1), 197–202 (2008).

[23] D. Pokrajac, T. Vance, A. Lazarević, A. Marcano, Y. Markushin, N. Melikechi *et al.*, "Performance of multilayer perceptrons for classification of LIBS protein spectra," in *10th Symposium on Neural Network Applications in Electrical Engineering, NEUREL-2010—Proceedings* (IEEE, 2010), pp. 171–174.

[24] G. Lorenzetti, S. Legnaioli, E. Grifoni, S. Pagnotta, and V. Palleschi, "Laser-based continuous monitoring and resolution of steel grades in sequence casting machines," Spectrochim. Acta, Part B **112**, 1–5 (2015).

[25] E. C. Ferreira, D. M. B. P. Milori, E. J. Ferreira, L. M. Dos Santos, L. Martin-Neto, and A. R. d. A. Nogueira, "Evaluation of laser induced breakdown spectroscopy for multielemental determination in soils under sewage sludge application," Talanta **85**(1), 435–440 (2011).

[26] E. D'Andrea, S. Pagnotta, E. Grifoni, S. Legnaioli, G. Lorenzetti, V. Palleschi *et al.*, "A hybrid calibration-free/artificial neural networks approach to the quantitative analysis of LIBS spectra," Appl. Phys. B **118**(3), 353–360 (2015), available from http://link.springer.com/10.1007/s00340-014-5990-z.

[27] Q. Shen, W. Zhou, and K. Li, "Quantitative analysis of Ni, Zr and Ba in soil by combing neuro-genetic approach and laser induced breakdown spectroscopy," Proc. SPIE **7854**, 78543Q (2010).

[28] J. M. Andrade, G. Cristoforetti, S. Legnaioli, G. Lorenzetti, V. Palleschi, and A. A. Shaltout, "Classical univariate calibration and partial least squares for quantitative analysis of brass samples by laser-induced breakdown spectroscopy," Spectrochim. Acta, Part B **65**(8), 658–663 (2010).

Published under license by AIP Publishing

[29]S. Pagnotta, M. Lezzerini, B. Campanella, S. Legnaioli, F. Poggialini, and V. Palleschi, "A new approach to non-linear multivariate calibration in laser-induced breakdown spectroscopy analysis of silicate rocks," Spectrochim. Acta, Part B **166**, 105804 (2020).
[30]B. Bhatt, A. Dehayem-Kamadjeu, and K. H. Angeyo, "Rapid nuclear forensics analysis via machine-learning-enabled laser-induced breakdown spectroscopy (LIBS)," AIP Conf. Proc. **2109**, 060006 (2019).
[31]A. Kumar Myakalwar, N. Spegazzini, C. Zhang, S. Kumar Anubham, R. R. Dasari, I. Barman *et al.*, "Less is more: Avoiding the LIBS dimensionality curse through judicious feature selection for explosive detection," Sci. Rep. **5**(1), 13169 (2015).
[32]Y. Liao, Y. Fan, and F. Cheng, "On-line prediction of pH values in fresh pork using visible/near-infrared spectroscopy with wavelet de-noising and variable selection methods," J. Food Eng. **109**(4), 668–675 (2012).
[33]W. Cai, Y. Li, and X. Shao, "A variable selection method based on uninformative variable elimination for multivariate calibration of near-infrared spectra," Chemom. Intell. Lab. Syst. **90**(2), 188–194 (2008).
[34]A. Safi, B. Campanella, E. Grifoni, S. Legnaioli, G. Lorenzetti, S. Pagnotta *et al.*, "Multivariate calibration in laser-induced breakdown spectroscopy quantitative analysis: The dangers of a 'black box' approach and how to avoid them," Spectrochim. Acta, Part B **144**, 46–54 (2018).
[35]U. Panne and K. Niemax, "Fifth international conference on laser-induced breakdown spectroscopy (LIBS 2008)," Spectrochim. Acta, Part B **64**, 929–930 (2009).
[36]S. M. Zaytsev, A. M. Popov, E. V. Chernykh, R. D. Voronina, N. B. Zorov, and T. A. Labutin, "Comparison of single- and multivariate calibration for determination of Si, Mn, Cr and Ni in high-alloyed stainless steels by laser-induced breakdown spectrometry," J. Anal. At. Spectrom. **29**(8), 1417–1424 (2014).

Published under license by AIP Publishing